

MICROERA POWER – ENHANCING THERMAL ENERGY STORAGE INSTALLATION EFFICIENCY

Kaela Brunner

Kyle Christensen

William Shaw

ABSTRACT

The global transition to renewable energy is challenged by the intermittency of energy source outputs, such as solar and wind, that do not offer the same reliability as fossil-fuel based energy generation. Variability in this generation results in uncertainties for customers, especially during times of peak demand. MicroEra Power's THERMAplus system offers a promising solution by providing efficient energy storage that allows customers to purchase electricity during times of low demand through the utilization of phase change material. The current system faces challenges with installation efficiency and overall layout. This project aims to redesign the system to be more mobile and standardized, optimize component layouts and improve the space efficiency. Advancements in these areas will facilitate broader adoption and ease the implementation of THERMAplus, supporting a more sustainable energy future.

PROBLEM DEFINITION

The transition to renewable energy is hindered by the variable output of renewable energy sources like solar and wind power. Solar energy is only available during daylight hours and is affected by cloud cover, while wind energy depends on weather conditions. In contrast, fossil fuel-based power plants provide steady, predictable electricity output, making them more attractive to grid operators despite their negative environmental impact.

This variability in renewable energy generation leads to fluctuating electricity prices, creating uncertainty for industrial and residential grid electricity consumers who must purchase electricity at higher peak-hour rates to maintain operations or lifestyle. The lack of an affordable and effective energy storage solution prevents consumers from capitalizing on lower off-peak rates and discourages further integration of renewables into the power grid. This, in turn, slows the global shift away from fossil fuels, exacerbating climate change and energy insecurity.

The MicroEra Power THERMAplus system addresses this issue by providing an efficient thermal energy storage solution. It effectively allows consumers to purchase electricity during off-peak hours, store it as thermal energy, and use it during peak-demand periods when electricity is more expensive. Over long-term operation, this system can lead to significant cost savings and reduce the grid's reliance on fossil fuels by making renewable energy more economically viable and predictable.

Widespread adoption of this technology could stabilize energy prices, enhance grid efficiency, and accelerate the world's transition to a sustainable energy future.

The current THERMAplus system faces challenges with installation efficiency. The goal of this project is to design a more modular and standardized system to address this, while also optimizing the piping and component layout of this system to minimize pressure and thermal losses during operation. The new system will also utilize a single reversible heat pump rather than a heat pump and chiller in combination to maximize space efficiency.

REQUIREMENTS, SPECIFICATIONS, DELIVERABLES

TABLE 1
PROJECT REQUIREMENTS

REQUIREMENT NUMBER	DESCRIPTION
1	The modular design must allow for easy access to all critical components. Critical components include valves, heat exchangers and pumps.
2	The design must have 3 separate piping loops, one for the heat pump sources, one for the building connection and one for the thermal energy storage (TES).
3	The heat pump must have 2 sources for connection and use.
4	For the case of system operation with no TES, the building loop must be on the supply side of the heat pump and the TES loop on the source side of the heat pump.
5	For the case of system operation with TES as a source, the building loop must be on the supply side of the heat pump and the TES loop on the source side of the heat pump.
6	For the case of system operation with direct heating/cooling with the TES, the TES loop must exchange with the building loop.
7	For the case of system operation with the TES being charged, the TES loop must be on the supply side with sources on the source side of the heat pump.

TABLE 2
PROJECT SPECIFICATION QUANTITIES

SPECIFICATION NUMBER	NUMBER VALUE	UNITS
1	48	inches
2	40	inches
3	72	inches
4	5	%
5	24	gal/min
6	4	hours
7	8	hours
8	3	°C
9	3	feet

TABLE 3
PROJECT SPECIFICATION DESCRIPTIONS

SPECIFICATION NUMBER	DESCRIPTION	METHOD OF EVALUATION
1	Maximum length allowed for system design (standard pallet dimension).	Tape measure
2	Maximum width allowed for system design (standard pallet dimension).	Tape measure
3	Maximum height allowed for system design.	Tape measure
4	An efficiency target for pump losses. Losses must be less than or equal to 5% of the total stored energy amount.	Spreadsheet calculation
5	System flow rate quantity. Based on previous TES charging and discharging measurements.	Purchased product specification
6	Heat transfer discharge rate based on a 150-gallon volume TES system.	Computation
7	Heat transfer charge rate based on a 150-gallon volume TES system.	Computation
8	Maximum temperature change allowed for the heat exchanger.	Purchased product specification
9	Piping connections to the TES system must be at least 3 feet above the base of the design.	Tape measure

TABLE 4
PROJECT DELIVERABLES

DELIVERABLE NUMBER	DESCRIPTION
1	A built prototype system that demonstrates the capability to meet the requirements and specifications.
2	A detailed report including all findings and simulation results.
3	A theory of operation manual that includes detailed explanations for running and maintaining the system.
4	A CAD package with a detailed bill of materials.

CONCEPTS

Shown below in Table 5 is a concept selection Pugh Matrix that was used to begin the overall system modeling. A baseline model (Figure 1, Appendix A) was considered and is a preliminary system sketch. For this sketch, and all other sketches considered, not all components included in the drawing are included in the current modular system. These sketches served only to clarify how components are connected and assisted with decision making regarding general valve, pump, and heat exchanger placement. Design 1 in Table 5 (Figure 2, Appendix A) is an alternative sketch of the system with key differences being a full building loop and the TES loop being connected on either side of the heat pump. Design 2 of Table 5 (Figure 3, Appendix A) is another iteration, and Design 3 (Figure 4, Appendix A) is the design that was used to begin component layouts. Criteria considered for the Pugh Matrix are that the design meets the requirements of the four different cases, has all required components, complexity, cost, and functionality. For the design to meet the requirements of the four different cases, these are, as described in Table 1, requirements 4 through 7. For the design having all required components, this refers to those listed as critical components in requirement 1 of Table 1. Complexity refers to how many components the design has, and how complicated it may be to create in both CAD and as a physical prototype as compared to the baseline. The cost is considered as a function of the amount of components (ex. valves), and the amount of time required to create the design. The functionality refers to whether the system is likely to perform the purpose of having a viable design of a modular THERMAplus system when compared to the baseline.

TABLE 5
CONCEPT SELECTION PUGH MATRIX

CRITERION	BASELINE	DESIGN 1	DESIGN 2	DESIGN 3
Meets requirements of the 4 different cases	0	-	-	+
Has all required components	0	-	+	+
Complexity	0	-	-	-
Cost	0	-	-	-
Functionality	0	+	+	+
Total	0	-3	-1	+1

The concept selection Pugh Matrix showed the team that Design 3 was the best to move forward with. Not only did the design have all the necessary components and adequate functionality, but it fully met all four of the case requirements set out at the start of the project. Design 3, as seen in Appendix A, Figure 4, was approved by MicroEra swiftly and contains three main loops for assembly. The first loop is the loop that connects sources 1 and 2 to the rest of the system. Sources 1 and 2 are natural sources of energy, for example, a small-scale solar setup or a geothermal loop. The second loop is the loop that connects necessary piping routes to the thermal energy storage, and the final loop connects to a building, such as a warehouse or home. From here on out these three loops will be referred to as the source loop, the thermal energy storage (TES) loop, and the building loop, respectively. Each loop serves a different function depending on the case that the overall system is operating under. Models and concepts of the overall design for each case and requirement have been made and can be seen in Appendix A, Figures 5-8.

Shown below in Table 6 is another concept selection Pugh Matrix, which is based on CAD modeling done after the implementation of Design 3 in Table 5. The matrix shows multiple possible design options for the overall system and component layout. Key characteristics of the designs include the total head loss in each loop calculated using Bernoulli's principle and Darcy-Weisbach, accessibility for maintenance, and the use of reservoirs for pump priming. Additionally, the system's ability to satisfy each of the heating and cooling subcase requirements was a critical consideration in each of the possible design options.

The first option, shown in Appendix A, Figure 9 uses the Grundfos UPS 43-100 SF pump in each of the three loops, as it served as a general placed holder while the head losses for the system could be determined along with the corresponding required pump head to power each of the loops at the required flow rate of 24 gallons per minute. This design serves as the baseline in the concept selection matrix shown in Table 6. After

further analysis, it was determined that these pumps lacked the power to drive flow in the system at the required flow rate. In this design, the pumps are elevated above the ground. However, this would likely be an unstable configuration and would exacerbate any vibrations in the system. It would also require heavy duty support to hold each of the pumps that would take up critical space from the rest of the components.

The second option shown in Appendix A, Figure 10 features the much larger and more powerful Dayton 4UA67 pump for the source and building loops and the 4UA65 for the thermal energy storage loop. The pump reservoir was omitted in this design due to the ability of both pump types to self-prime, greatly simplifying piping layout and increasing accessibility to critical components for maintenance.

The third and final design, shown in Appendix A, Figure 11 was very similar to the second. However, a change was made to the location of a valve in the source loop to ensure proper operation in each of the heating and cooling subcases and system supports were added. The valve was moved from the outlet of the pump to the outlet of the heat exchanger.

TABLE 6
CONCEPT SELECTION PUGH MATRIX

CRITERION	BASELINE	DESIGN 1	DESIGN 2
Meets requirements of the 4 different cases	0	-	+
Head loss	0	+	+
Accessibility	0	+	+
Total	0	+1	+3

According to this concept selection matrix the final decision was made to move forward with Design 2, as it was the most optimized for pressure loss, satisfied all subcase criteria, and had the highest degree of accessibility for maintenance. Detailed CAD drawings of the overall finalized assembly and each of the three loops can be seen in Appendix C, Figures 1-4.

MECHANICAL ANALYSIS

Tolerance Analysis

For proper fabrication and operation, the ports of the heat exchangers must be in the correct location so that they can be securely fastened to their associated pipe terminations. Therefore, it was necessary to perform a tolerance analysis on the heat exchanger stand where the critical dimensions are shown in Appendix B, Figure 1 as A, B and C, where the nominal value for B, to ensure a correct fit, is the desired output from the analysis and the location of the heat exchanger is assumed to be fixed at 6.75 inches.

Using a worst-case analysis, the minimum length of B is shown in Equation 1 below and was found to be 5.23 inches:

$$B_{min} = 6.75 - A_{max} - C_{max} \quad (1)$$

Given that the tolerance of B is 0.01 inches, the nominal value of B is 5.24 inches. Therefore, the length of 5.24 ± 0.01

inches ensures the bottom of the heat exchanger is at 6.75 inches or below.

Fatigue Analysis

The components of the system most vulnerable to fatigue failure are the metal straps securing each of the heat exchangers to their stands. The straps are perforated galvanized steel and are 0.75 inches by 0.047 inches in cross-section [1].

The straps are subjected to vibration-induced cyclical loading at 57.5 Hz from pump operation. To ensure fatigue failure will not occur, a fatigue analysis was performed according to the loading conditions. Conservative estimates for all material properties were used. The ultimate tensile strength, S_U , was considered to be 400 MPa, the yield strength, S_Y , was considered to be 220 MPa, the endurance limit, S_e' , was considered to be 200 MPa, which is half of the ultimate strength, as S_U is less than 1400 MPa [2].

Again, to provide a conservative estimate, the strap was assumed to be prestressed with the minimum stress during a cycle being zero, and the maximum stress to be the sum of the prestressed value and the amplitude of the stress due to vibration. The pre-stress S_m was estimated to be 8.8 MPa using 200 N over the cross-sectional area of the strap as that is approximately the force a human can exert on the strap in tension during installation. S_e was calculated to be 137 MPa according to the following equation:

$$S_e = K_a K_b K_c K_d K_e K_f S_e' \quad (2)$$

where K_a is the surface condition modification factor and was calculated to be 0.86 according to the following equation:

$$K_a = a S_U^b \quad (3)$$

where a and b are 0.83 and -0.265 respectively and are empirical constants unique to the material and surface finish from Table 6-2 in Shigley's Mechanical Design [3]. K_b is the size modification factor and was taken to be 1 because loading is axial. K_c is the load modification factor and was taken to be 0.86 because the straps are only loaded axially. K_d is the temperature modification factor and was calculated to be 1 according to the following equation:

$$K_d = 0.975 + 0.432(10^{-3})T_F - 0.115(10^{-5})T_F^2 + 0.104(10^{-8})T_F^3 - 0.595(10^{-12})T_F^4 \quad (4)$$

Where T_F is the ambient temperature, which was taken to be 70 degrees Fahrenheit. K_e is the reliability factor and was calculated to be 0.93 using the following equation:

$$K_e = 1 - 0.08z_a \quad (5)$$

where z_a is the transformation variable that is dependent on the reliability percentage or the analysis. In this analysis the reliability percentage was taken to be 95%, meaning z_a was 0.868 according to Table 6-5 in Shigley's

Mechanical Design [3]. K_f is the miscellaneous effects modification factor and was assumed to be 1.

While the actual stress due to vibration experienced by the straps is unknown, it can be estimated using Equation 6 below and was calculated to be 1.67MPa:

$$S_a = \frac{m(2\pi f)^2 x}{A} \quad (6)$$

where x is the amplitude and was estimated to be 0.25 mm, f is the frequency of vibration, and m is half the mass of the heat exchanger being held in place or 1.17 kg.

The fatigue state was determined using the ASME elliptical criteria using Equation 7 below and was calculated to be 0.00175. This value is far less than 1, indicating that there is very little risk of fatigue failure in the heat exchanger straps.

$$1 = \left(\frac{S_a}{S_e}\right)^2 + \left(\frac{S_m}{S_y}\right)^2 \quad (7)$$

All equations in this section are from Shigley's Mechanical Design [3].

Fastener Torque Calculation

The carriage bolts that hold the pumps to the plywood sheath are vital components. It is assumed that the bolts are 6mm nominal diameter, class 4.6, and zinc plated. To calculate the proof load, the following equation is used:

$$F_p = A_t S_p \quad (8)$$

where A_t is the tensile stress area in mm² and S_p is the proof strength in MPa. Values for tensile stress area and proof strength come from Table 8-1 and Table 8-9 of Shigley's Mechanical Design, respectively [3]. The equation for preload for a nonpermanent connection is seen in Equation 9.

$$F_i = 0.75F_p \quad (9)$$

Lastly, the torque equation is seen in Equation 10.

$$T = K F_i d \quad (10)$$

where K is the torque factor and d is the nominal major diameter. The torque factor is found from Table 8-15 of Shigley's Mechanical Design [3]. The required torque was calculated to be approximately 3.98 lb_f · ft. Knowledge of the required torque of these bolts is important, especially considering the vibrations generated by the pumps.

Material Selection

When deciding which type of plastic piping to use within the system, there were two viable options: crosslinked polyethylene (PEX) and polypropylene (a popular brand being Aquatherm). PEX was chosen over Aquatherm based on advice

from the sponsor. PEX is corrosion resistant, which is vital, as the TES may have corrosive fluids running through it. Furthermore, PEX is widely available for purchase. Specifically, the system uses PEX-B, which is the most common type of PEX, making it easy to acquire. PEX-B is formed using a silane cross linking method [4]. PEX-B has a tensile strength of greater than or equal to 20 MPa [5].

Computer-Based Analysis

To inform the design of the system, a modal analysis was performed on the stands supporting the heat exchangers. The pumps used in the system operate at 3450 RPM and apply vibrations to the entire system at this frequency. It is critical that the resonant frequencies of the system and of the components within the system, such as the heat exchanger, stands, supports, and tubing, do not match the operational frequency of the pumps so that the risk of catastrophic failure of the system is minimized. A resonant frequency that is close to the pump operational frequency would greatly quicken the rate of fatigue onset.

The heat exchanger stands were determined to be the most critical component of the system regarding vibration and fatigue onset because they have the least damping ability and are connected directly to the base, where vibration energy is greatest. They are also the most critical components to the system's successful operation.

The rotation of the pump motors is oriented about the Y axis of the system, and so the largest vibration amplitude applied on the system by the pumps would be in the X-Z plane. As such, the orientation of the main back plate of the heat exchanger stand was chosen to maximize the area moment of inertia (according to Equation 11) in that direction in order to minimize the stands susceptibility to bending in that direction due to vibration. Similarly, supports were added in the Y-Z plane in order to add resistance to bending in that direction.

$$I = \left(\frac{1}{12}\right)bh^3 \tag{11}$$

To ensure the resonant frequency of the heat exchanger stands did not match the frequency of the pumps, a vibration analysis was conducted on the structure in Siemens NX using NASTRAN Solution 103 – Real Eigenvalues. A finite element analysis model was created using a two 3D tetrahedral meshes. The stand itself is made completely of plywood and therefore was given a modulus of elasticity of 1000000 psi (the most conservative estimate), a mass density of 0.025 lb/in³, and a Poisson's ratio of 0.33. The plywood mesh had an element size of 0.4 inch, which is a sufficiently small resolution to yield accurate results for a geometry without curves. The heat exchanger was modeled as a 3D tetrahedral mesh as well, but with a smaller element size of 0.1 inch to accurately capture the curvature. The heat exchangers are made mostly of stainless steel but are brazed with copper. In the simulation, the heat exchanger was modeled completely as stainless steel because there is little deformation in the heat exchanger relative to the wooden stand due to the stark

difference in stiffness between the two structures. A fixed restraint was placed on the entire bottom surface of the stand to replicate the screws securing the stand to the base of the system. No constraints were placed on the ports of the heat exchanger where the pipes connect because the pipes are not significantly stiff and allow small amounts of motion in all directions. The FEA model set up is shown in Figure 1.

The resulting eigenvalues from the analysis and their corresponding stresses are shown in Table 7. Each eigenvalue corresponds to a resonant frequency of the structure. Modes 2 and 3 are most critical as they are closest to the pump operational frequency of 3450 RPM or 57.5 Hz. However, these frequencies are different enough that resonance will not occur. As a result, the structure is optimized to minimize fatigue and maximize the longevity of the system. The structure and its elemental scalar strain energy for modes 2 and 3 are shown in Appendix B, Figures 2 and 3 at maximum deformation. If one of the resonant frequencies from the analysis matched the pump frequency or was close, the structure would have needed to be redesigned to avoid failure because of resonance.

TABLE 7
VIBRATION ANALYSIS RESULTS OF HEAT EXCHANGER STAND

VIBRATION MODE	EIGENVALUE (Hz)
1	27.35
2	29.24
3	76.19
4	205.28
5	242.99
6	262.12
7	845.95

A second vibration analysis was conducted on what was determined to be the most vulnerable section of pipe to vibration and fatigue. The analysis was performed in NX as well, using NASTRAN Solution 103 – Real Eigenvalues. A mesh was created using 20 c-beam elements of tubular cross section with inner diameter 0.875 inches and outer diameter of 1.125 inches to ensure sufficient resolution, using conservative material properties of PEX B piping. The resonant frequencies from this analysis can be seen in Table 8, the most concerning of which are mode 2 and 3. However, they are not close enough to the pump frequency to pose a risk of resonance and subsequent fatigue failure of the pipe or the cross connection. The vibrational modes can be seen below in table 8, and the FEM setup, and strain energy plots of modes 2 and three can be seen in Appendix B, Figures 4,5 and 6.

TABLE 8
VIBRATION ANALYSIS RESULTS OF HEAT EXCHANGER STAND

VIBRATION MODE	EIGENVALUE (Hz)
1	29.38
2	33.20
3	98.38
4	115.08
5	281.33
6	305.53
7	348.67

Fundamental Mechanical Analysis

Pressure drop and head loss calculations were completed separately for each of the three loops of the system using a MicroEra-provided Google Sheets spreadsheet and a team-created Python code. The code can read in lengths of space reservations for each section of tubing in each loop, taken from an NX-created Excel spreadsheet, and then convert the lengths from inches to feet. Lastly it will input those lengths into the corresponding positions in the loss calculations spreadsheet. For further information on how the code is used, see the ‘TeamMicroEraProgramTheoryOfOperation’ document.

The loss calculations spreadsheet uses Bernoulli’s principle and the Darcy-Weisbach equation, with inputted lengths, flow rate, fluid information, pipe fittings, and PEX piping properties. The equation used within the Google spreadsheet is given by Equation (12):

$$\Delta P = \frac{f}{2d} \rho v^2 + \sum_1^N \frac{K_n}{2} \rho v^2 + \frac{1}{2} \rho (v_2^2 - v_1^2) + \rho g (h_2 - h_1) \quad (12)$$

where f is the Darcy friction factor, v is the flow velocity, K is the loss coefficient associated with turns, h is the flow’s height, ρ is the density, g is the acceleration due to gravity, and d is the diameter of the pipe.

Head loss and pressure drops were calculated for each loop in their entirety, in addition to each subcase of each loop, for multiple iterations of CAD designs. The original and final values can be seen in Table 1 of Appendix A, with the original calculations corresponding to the baseline as shown in Figure 9 in Appendix A, and the final calculations corresponding to Design 2 as shown in Figure 11 of Appendix A. The different subcases of each loop can be seen in Table 2 of Appendix A. The highest subcase value of head loss calculated for each loop was used to purchase pumps.

MANUFACTURING

PEX-B is used for the designed system’s piping, as described in the Material Selection of the Mechanical Analysis Section. For the heat exchanger supports, 23/32-inch plywood was used, due to cost considerations, ease of manufacturing, and time limitations. The plywood sheet was purchased as a base to lie on the underlying pallet. Leftover plywood was used to stretch the budget further. Furthermore, team members have

experience with basic woodworking, so assistance was not needed, and creation of the part could be completed outside of typical shop hours. As for PEX piping supports, polyvinyl chloride (PVC) piping is used for its rigidity and ease of manufacturing.

An estimate of the associated costs of the system production is approximately \$9,300, calculated by adding hardware costs, seen in Tables 9 and 10, and build time costs at \$100/hr per person, seen in Table 12. Development costs for the system are approximately \$30,500, as seen in Table 11.

If the system were to be scaled to 1,000 systems, there are multiple changes that could be made to improve cost and build time. Primarily, purchasing straight PEX instead of coiled PEX would result in improvements. Straight PEX would allow for a build process more like an assembly line, as there would be less room for error when cutting pipe lengths to size. The current build method of putting the pipes together was not efficient. This is due to the fact that the PEX piping could not be cut all in one go, because real-time edits to lengths were necessary to compensate for the curvature of the pipes. Next, the PEX piping supports could likely be improved to decrease costs and build time. It may be beneficial to design and mold flanged fittings to fit the 2-inch PVC pipe, instead of purchasing bushings to fit the pipe into a 3-inch toilet flange (as there does not seem to be an existing product for a 2-inch flange fitting).

TABLE 9
PURCHASED HARDWARE COST ESTIMATE TABLE

ITEM	QUANTITY	TOTAL COST
Tee Connectors	6	\$29.22
90 Degree Elbow Bends	30	\$130.80
4 Pack of Ball Valves	1	\$29.99
10 Pack of Ball Valves	1	\$64.88
6 Pack of 1-inch Pipe Adapters	2	\$39.98
8 Roll Teflon Tape	1	\$7.99
100 feet of 1-inch PEX Piping	1	\$85.19
Pipe/Tube Reamer	1	\$6.99
10 Pack of 1-inch Clamps	1	\$11.59
1.5-to-1-inch NPT Bushings	6	\$29.76
1 inch NPT to 1-inch Barbed Adapter	6	\$59.88
1 sheet of Plywood 23/32-inch thick	1	\$41.00
Extension Cords 12 Wire Gauge	3	\$59.01
Cross Connectors	2	\$11.86
100 Pack of 1-inch Clamps	1	\$87.33

Flexible Strap Support Hanger	2	\$9.94
Water Conduit Connectors	3	\$8.85
2-inch S-40 PVC	2	\$28.72
3-inch x 2-inch PVC DWV Flush Bushing	8	\$47.60
3 inch Outside Fit PVC Toilet Flange	8	\$44.48
25 Pack 1-1/2 Clamping Diameter Worm Gear Clamps	2	\$54.32
TOTAL PURCHASED HARDWARE COST		\$889.38

TABLE 10
SPONSOR PURCHASED HARDWARE COST ESTIMATE TABLE

ITEM	QUANTITY	TOTAL COST
Dayton Centrifugal Pump (90 feet max Head)	1	\$620.21
Dayton Centrifugal Pump (78 feet max Head)	2	\$1,122.98
Bell and Gossett Braze Heat Exchanger	2	\$898.98
TOTAL SPONSOR PURCHASED HARDWARE COST		\$2,642.17

TABLE 11
DEVELOPMENT TIME COST ESTIMATE TABLE

MEMBER	HOURS	COST
Kaela Brunner	99.3	\$9,930
Kyle Christensen	101.2	\$10,120
William Shaw	104.5	\$10,450
TOTAL DEVELOPMENT COST		\$30,500

TABLE 12
BUILD TIME COST ESTIMATE TABLE

MEMBER	HOURS	COST
Kaela Brunner	22.5	\$2,250
Kyle Christensen	19.5	\$1,950
William Shaw	16	\$1,600
TOTAL BUILD COST		\$5,800

TEST PLAN AND RESULTS

Each specification for this system, which can be seen above in Tables 2 and 3, was tested and reported as either passed or failed in Table 13 below. There were no modifications made to any of the requirements or specifications from the original set that was agreed upon by the team and the sponsor.

TABLE 13
SYSTEM SPECIFICATION PASS/FAIL

SPECIFICATION NUMBER	PASS/FAIL
1	PASS
2	PASS
3	PASS
4	FAIL
5	FAIL
6	PASS
7	PASS
8	PASS
9	PASS

Specifications 1, 2, 3 and 9 all passed and were measured using a standard tape measure. The first two specifications are the dimensions of a standard pallet, which made acquiring a correctly sized pallet an easy task. As for specification 3, the highest distance from the base of the system that a component reaches are just over 3 feet, thus meaning this specification passed. Specification 9 required that connections to the TES loop be above 3 feet off the base of the system, and the connections are at 3.25 feet, meaning that this specification was met. Specifications 8 also passed by ensuring that the purchased components achieved the required temperature change. The heat exchangers purchased adhere to a maximum temperature change of 3°C, successfully meeting specification 8. The water heat dissipation capacity was calculated using the following equation:

$$\dot{Q} = \dot{m}c\Delta T \quad (13)$$

where \dot{m} is the flow rate, given by the 24 gallons of water per minute, C is the specific heat capacity of water, and ΔT is the maximum temperature change of 3°C. The heat dissipation capacity required that was calculated was approximately 64,000 Btu/hr. Heat exchangers with 150,000 Btu/hr water heat dissipation capacity were purchased. Similarly, specifications 6 and 7 were also met by ensuring that the purchased heat exchangers could sufficiently meet the charge and discharge rates. Given a TES system of approximately 150 gallons and 300 MJ/m³, a 4-hour discharge rate requires a minimum of about 40,300 Btu/hr, and an 8-hour charge rate requires a minimum of about 20,200 Btu/hr. Thus, these specifications are met by the 150,000 Btu/hr heat exchangers that were purchased.

As for Specification 4, it unfortunately failed. This specification requires an efficiency target of less than or equal to 5% of the total stored energy amount, the 135 MJ of the TES system, considering both the charge and the discharge rates of the system. For the 4 hour discharge rate, the needed power consumption would need to be less than approximately 469 W. The actual required power consumption of the 3 pumps given the calculated final pressure drops of CAD Design 2 (Figure 11 in Appendix A) is about 1798 W. As for the 8 hour charge rate, the needed power consumption would need to be less than approximately 234 W. The actual required power consumption is approximately 1700 W. The actual power consumption rates

clearly do not meet the requirements of Specification 4, likely due to the inefficiency of the Dayton Pumps. The motor efficiency, as given on the motor plates, is 55%, which is lower than typical.

Specification 5 – the flow rate must be 24 gallons per minute - was not met as well. This was determined for the source loop by measuring the time it took the discharge fluid of the loop to fill a 3.3-gallon bucket. The measured flow rate was approximately 6 gallons per minute which does not meet the required 24 GPM. It should be noted, however, that the pressure drop and flow rate analysis done previously was for a closed source loop, whereas the measurement was taken for an open loop. The open-loop effect greatly increases the flow energy lost and pressure lost as the pump must accelerate the inlet flow from zero. In reality, during operation, the flow rate would likely be much higher, approaching the 24 gallons per target.

For further validation, the pressure was measured at the pump outlet of the source loop. The measured pressure was 6 psi, which was far lower than our calculated pressure. This, again, is likely due to the measurement being taken on an open loop instead of a closed loop because all pressure achieved by the pump is lost when the flow enters the atmosphere.

INTELLECTUAL PROPERTY

The design is not patentable, as it draws upon existing MicroEra ideas. While the design has multiple differences from the current THERMAplus system, such as use of a heat pump or the condensed, modular nature of the system, the overall function is incredibly similar, and thus the system design is not novel.

Some existing patents within this field include: US11378282B2, US10663232B2, CN110129916A, and of course MicroEra's own patent: US11970652B1 [6]. Relevant companies and individuals in the realm of the thermal energy storage systems include: Climatewell Ab, Gree electric, and David Kreutzman [6].

SOCIETAL AND ENVIRONMENTAL IMPLICATIONS

The THERMAplus system has many potential societal and environmental impacts. The most impactful of which is the potential effects it has on enabling the use and further adoption of renewable energy sources such as wind and solar energy. Due to the highly variable nature of wind and solar energy output to the grid, adoption has been slow because of the greater reliability of alternative energy sources like fossil fuels and coal.

The THERMAplus system allows customers to mitigate their exposure to price fluctuations in electricity costs due to variations in demand and supply of electricity, effectively combating the main drawbacks of wind and solar energy. This could indirectly reduce greenhouse gas emissions due to the combustion of fossil fuels and slow the rate of climate change.

Additionally, thermal energy storage systems like this could improve energy equity in regions where there is no access to grid energy. Small, local solar or wind farms could be used to power facilities. Normally, the unpredictability of small-scale solar and wind farms makes them an unviable option in rural areas, as the need for electricity is constant, but the supply is

variable. With a system like THERMAplus, energy could be stored in excess during the day, or during windy times, and used later to guarantee a constant supply of power.

The manufacturing process for the system is not particularly energy-intensive, and any net energy costs for the process are offset by the resulting savings associated with the use of the system.

RECOMMENDATIONS FOR FUTURE WORK

The most critical and logical next step for the system's development is the automation of operation. Due to financial restraints on the budget for the project, the choice was made to use manual ball valves rather than electronic valves. However, for the system to be a viable product and operate successfully, control over the valves would need to be delegated to a computer system. The system would be able to control the correct valves according to the desired heating, charging, or cooling subcases. The system also should have the intelligence to determine which subcase should be executed using the current energy usage of the customer, cost of electricity, and internal and external temperatures as inputs to determine the most optimal choice.

Additionally, to make a more viable product, the manufacturing and fabrication processes should be streamlined to reduce fabrication and labor costs. Alternative components could be explored that would allow for manufacturing automation. For example, rather than using PVC and plywood for the supports, laser-cut sheet metal could be used. This would also increase consistency in the case where many systems are being made.

Furthermore, some components may need to be switched out for others, or adjusted. A key example is the 1.5-to-1-inch NPT bushings currently in the pump inlets and outlets. These bushings are made of black iron, which is typically meant for fittings of gas systems, and thus, they are likely to rust in the liquid system. This was unknown at the time of purchase, and so these bushings will likely need to be replaced with a rust-resistant material. Another example is the tightening or replacement of clamps within the system, especially in the building and TES loops, as to avoid leaking. Lastly, the pumps for the building and TES loops need to be primed before they are turned on.

Testing and analysis of any thermal losses in the system as well as heat transfer rate and heating and cooling ability, should be done to verify successful operation. Possible optimizations, such as pipe insulation, should be explored. Further optimization for pressure loss could be done to potentially reduce pump flow losses and overall efficiency.

The current system failed specification 4, which states that the pump losses must be less than or equal to 5% of the total stored energy amount. This is, in part, due to the pump motors being relatively inefficient. Their nominal efficiency is rated to be 55%. Typical pump motor efficiencies are above 80% so it would be worthwhile to explore alternative pumps with higher efficiencies to reduce pump losses.

Another critical aspect for a successful product launch is the system's longevity and accessibility to components for

maintenance. Further vibration analysis and optimization should be done to inform design and minimize damage due to fatigue.

ACKNOWLEDGMENTS

We would like to extend our sincerest gratitude to several individuals who have been instrumental in contributing to the success of this project.

Firstly, we would like to thank our sponsor, Molly Over, for her generous sponsorship, commitment, and valuable feedback throughout the duration of this project. We are greatly appreciative of her mentorship and commitment to our success with this project.

We would like to thank lab specialist Samantha Kriegsmann for her steadfast assistance and support with all things relating to the ins and outs of our system components.

We are immensely grateful to Bill Mildenerger for generously allowing us to utilize his workspace and tools in Taylor Hall.

We express great appreciation to Jim Alkins for contributing to the setup of the pumps for our system design and for generously allowing us to utilize his workspace in Rettner Hall.

We would like to extend our sincerest gratitude to Chris Pratt for her assistance on our MRR and for her exceptional efficiency in ordering and promptly acquiring our system components.

We would like to thank Alex Prideaux for his contributions in ordering and acquiring our system components and for being an ear of assistance to any questions we had.

We express great appreciation to our TA Sebastian Gomez for his time, dedication, and guidance throughout the entire duration of this project.

We express our deepest appreciation and gratitude to Professor Chris Muir for his unwavering support and guidance throughout this project. Professor Muir's dedication and wisdom have been greatly appreciated and instrumental in this project. We are greatly appreciative of his mentorship and commitment to our success as engineers.

REFERENCES

- [1] "McMaster-Carr." [Online]. Available: <https://www.mcmaster.com/3051T13/>. [Accessed: 26-Apr-2025].
- [2] "Overview of Materials for Low Carbon Steel." [Online]. Available: <https://www.matweb.com/search/DataSheet.aspx?MatGUID=034970339dd14349a8297d2c83134649&ckck=1>. [Accessed: 26-Apr-2025].
- [3] Budynas, R. G., Nisbett, J. K., and Shigley, J. E., 2015, *Shigley's Mechanical Engineering Design*, McGraw-Hill Education, New York, NY.
- [4] 2021, "The Differences Between PEX-A, -B and -C | SharkBite." [Online]. Available: <https://www.sharkbite.com/us/en/resources/blog/the-differences-between-pe-x-a-b-and-c>. [Accessed: 26-Apr-2025].

- [5] "Total Materia :: Mechanical Properties." [Online]. Available: <https://portal.totalmateria.com/en/search/quick/materials/5018016/mechanical>. [Accessed: 26-Apr-2025].
- [6] "Google Patents." [Online]. Available: <https://patents.google.com/>. [Accessed: 26-Apr-2025].

APPENDIX A – RELEVANT SYSTEM LAYOUTS AND TABLES

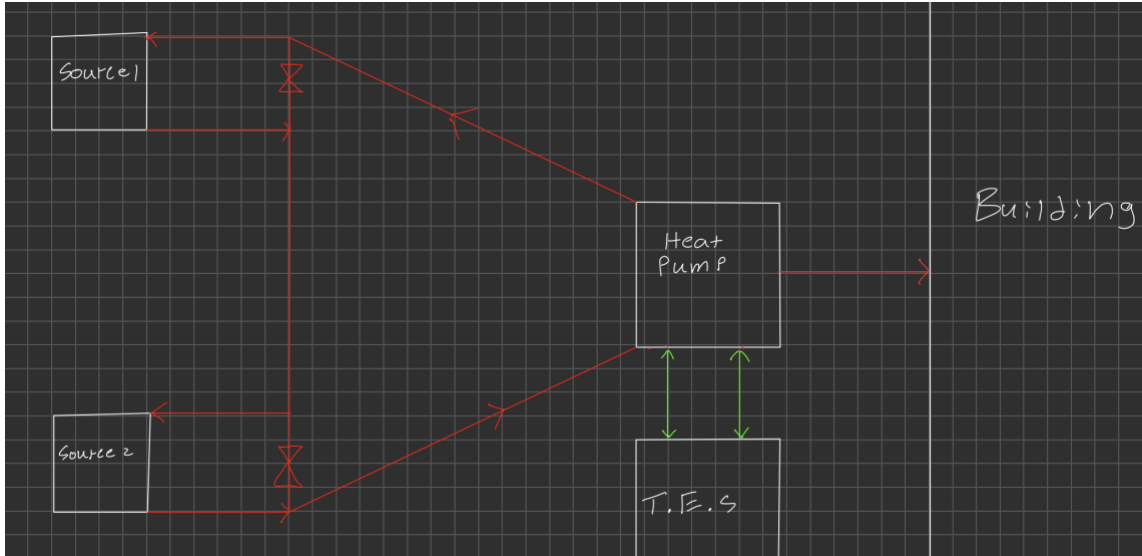


Figure 1. First preliminary system design sketch after initial meeting with MicroEra.

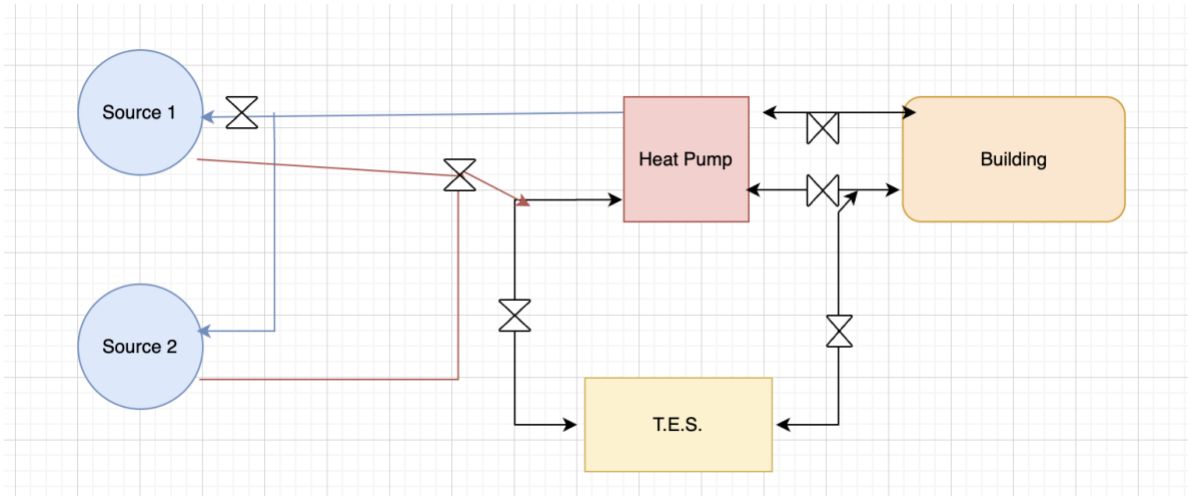


Figure 2. Preliminary sketch diagram of general system process.

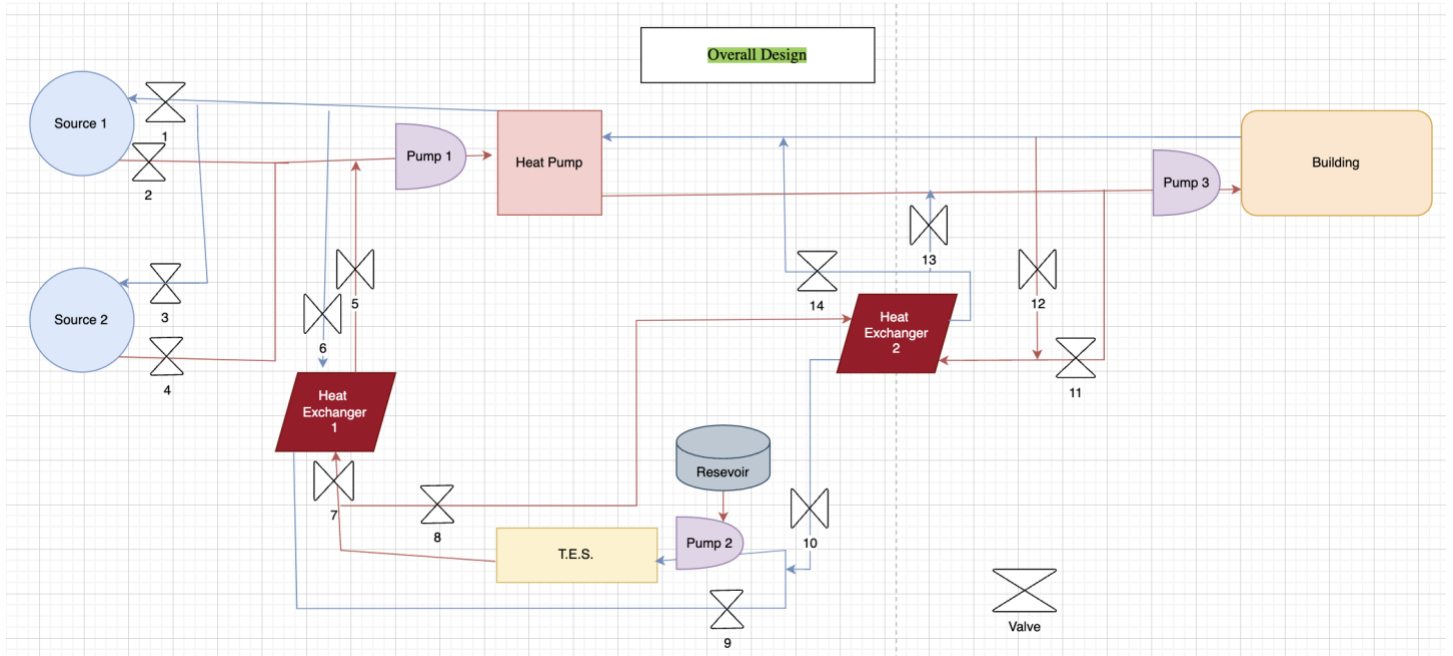


Figure 3. Iteration sketch diagram of overall system.

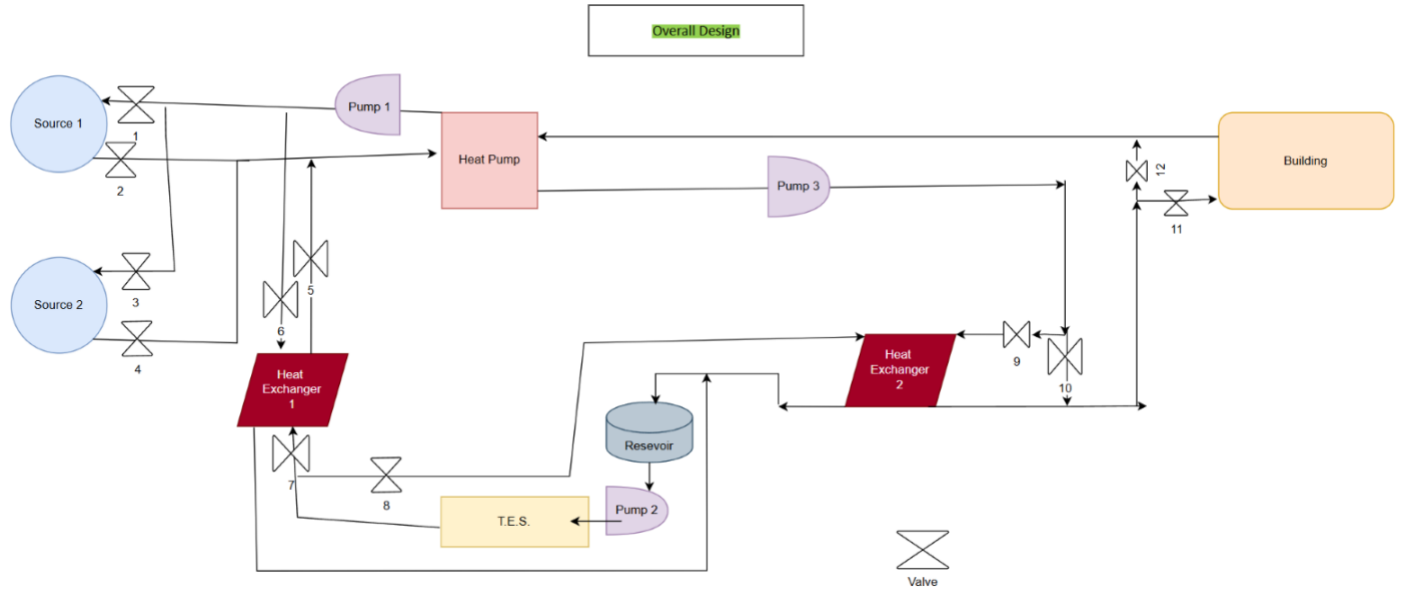


Figure 4. Optimum final design sketch of overall system after iterations and meeting all requirements.

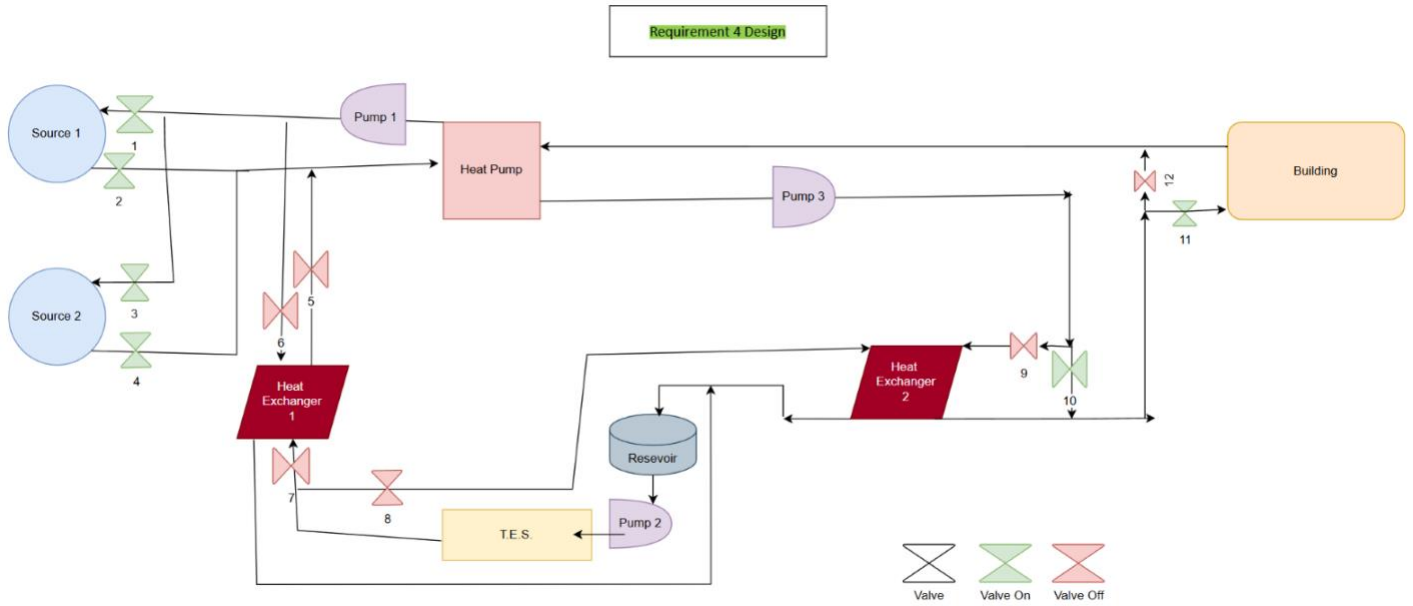


Figure 5. Final design sketch from Figure 4 for meeting Requirement #4.

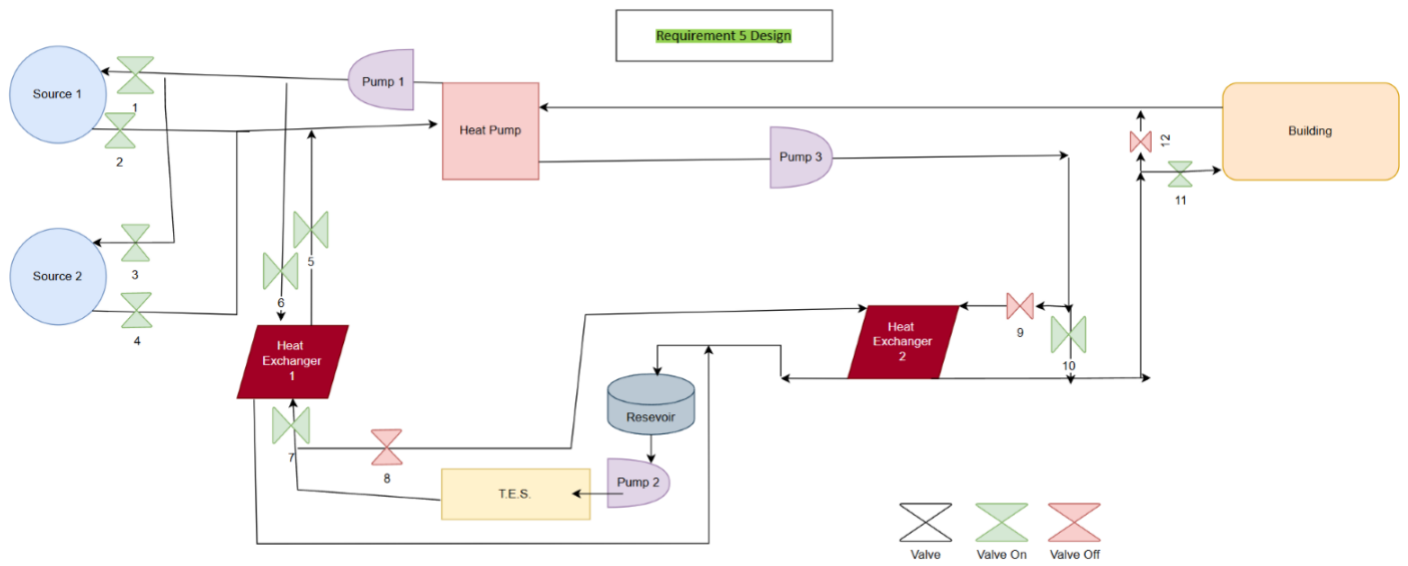


Figure 6. Final design sketch from Figure 4 for meeting Requirement #5.

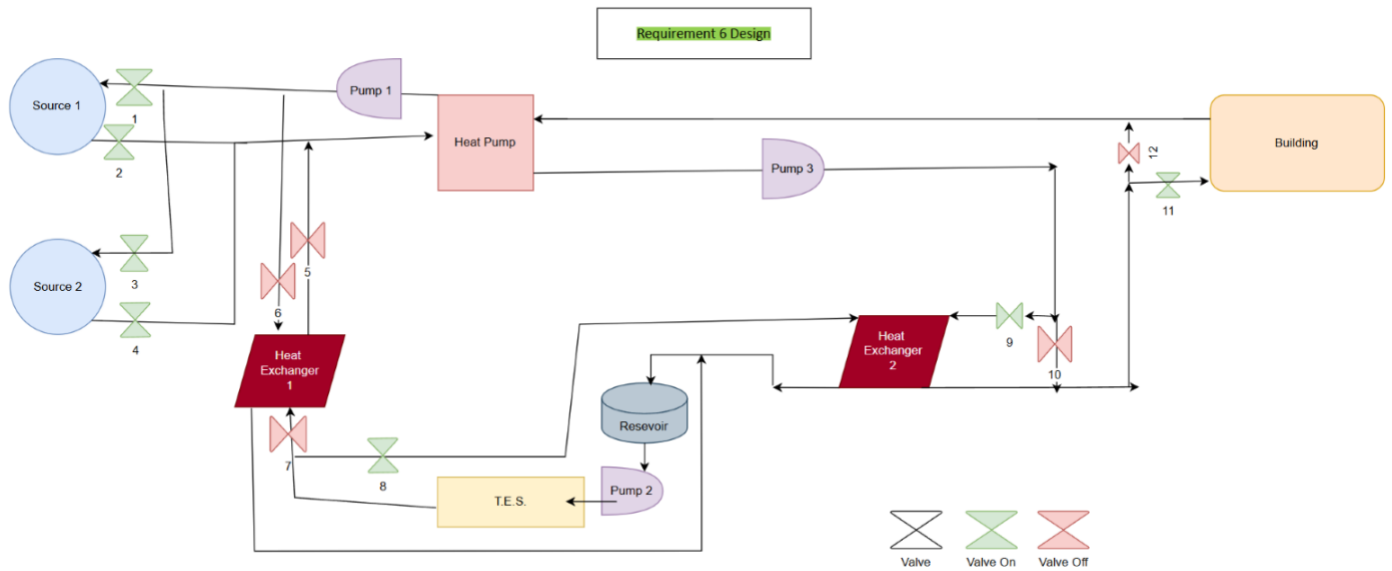


Figure 7. Final design sketch from Figure 4 for meeting Requirement #6.

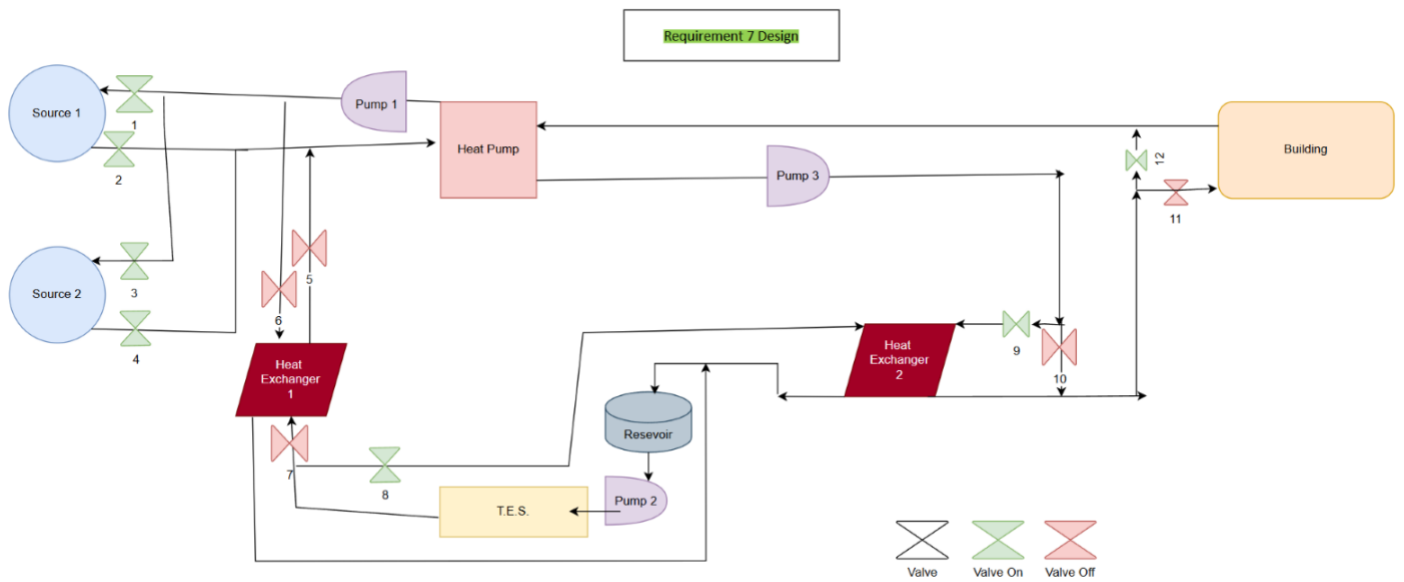


Figure 8. Final design sketch from Figure 4 for meeting Requirement #7.

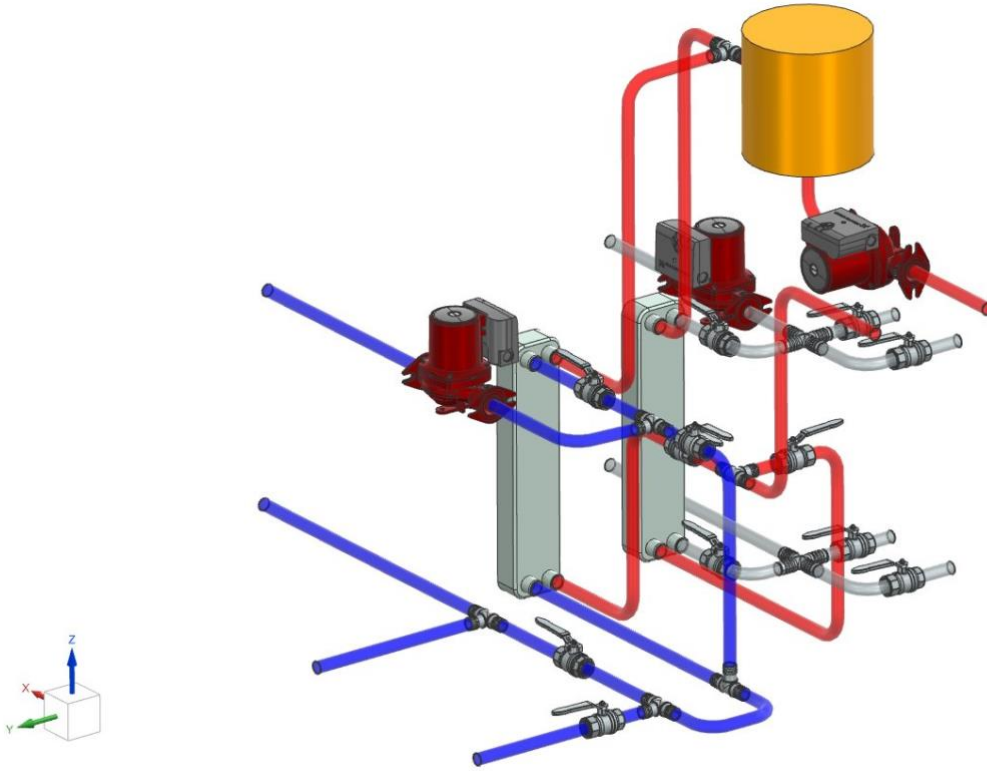


Figure 9. Initial design with suspended pumps (Baseline)

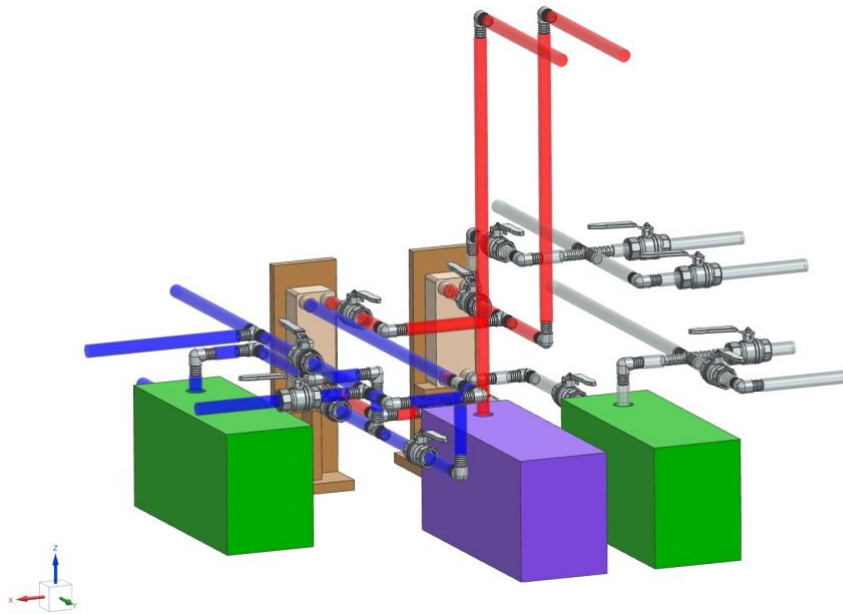


Figure 10. Updated design with grounded Dayton pumps (Design 1).

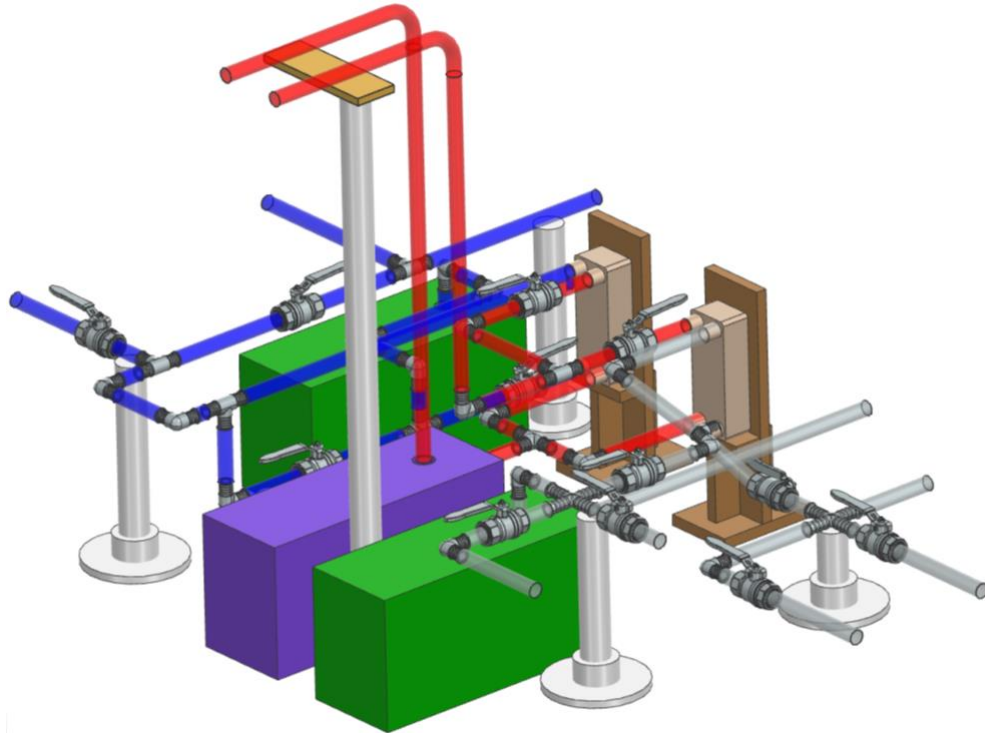


Figure 11. Final design with updated source loop configuration (Design 2)

TABLE 1
HEAD LOSS AND PRESSURE DROP CALCULATIONS

	ORIGINAL		FINAL	
	HEAD LOSS (ft)	PRESSURE DROP (psi)	HEAD LOSS (ft)	PRESSURE DROP (psi)
TES LOOP				
Overall	125.0	54.2	94.6	41.0
Subcase 1	72.1	31.3	56.3	24.4
Subcase 2	74.4	32.2	49.3	21.4
Subcase 3	-	-	-	-
BUILDING LOOP				
Overall	55.8	24.2	63.5	27.5
Subcase 1	30.8	13.4	37.4	16.2
Subcase 2	44.7	19.4	51.2	22.2
Subcase 3	39.7	17.2	46.6	20.2
SOURCE LOOP				
Overall	56.8	24.6	44.4	19.2
Subcase 1	56.8	24.6	44.4	19.2
Subcase 2	24.0	10.4	22.8	9.9

TABLE 2
SUBCASES OF LOOPS

	OPEN VALVE(S)	CLOSED VALVE(S)	REQUIREMENT(S) MET
TES LOOP			
Subcase 1	8	7	#6, #7
Subcase 2	7	8	#5
Subcase 3	-	7, 8	#4
BUILDING LOOP			
Subcase 1	10, 11	9, 12	#4, #5
Subcase 2	9, 11	10, 12	#6
Subcase 3	9, 12	10, 11	#7
SOURCE LOOP			
Subcase 1	1, 2, 3, 4, 5, 6	-	#5
Subcase 2	1, 2, 3, 4	5, 6	#4, #6, #7

APPENDIX B – VIBRATION ANALYSIS

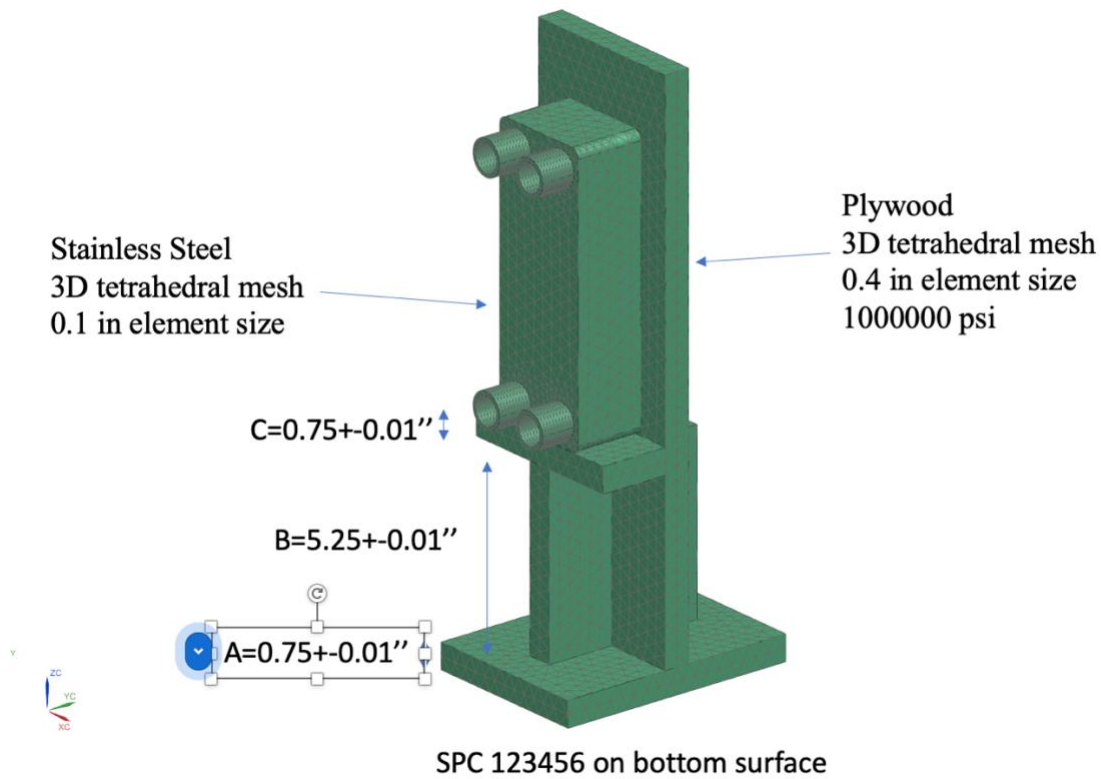


Figure 1. FEA of heat exchanger stand.

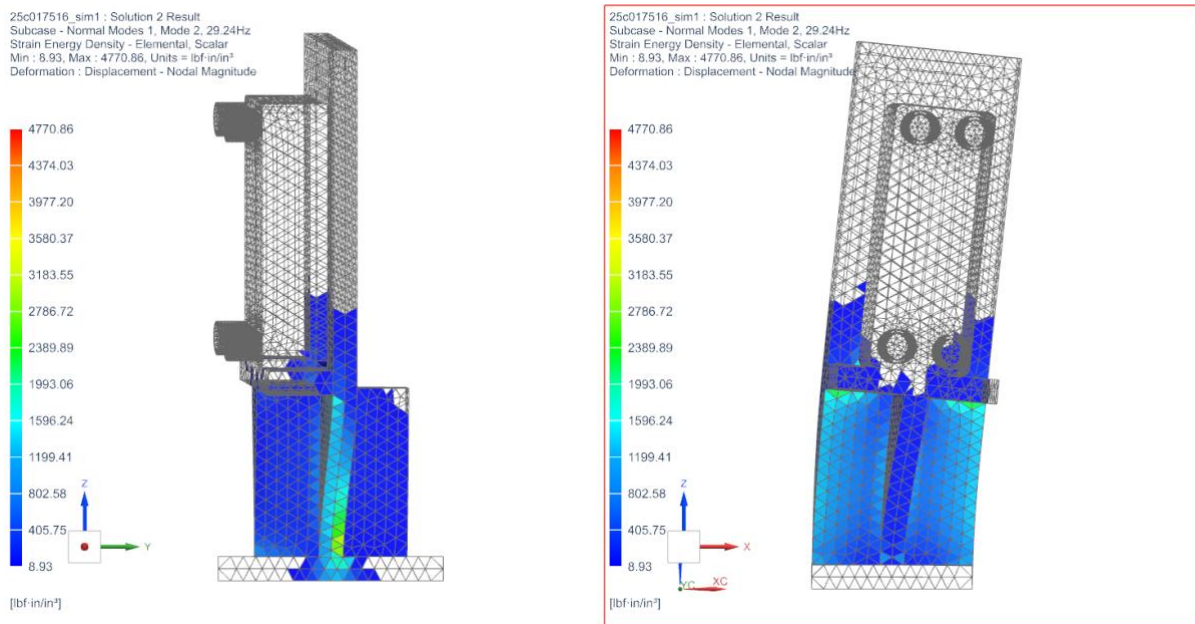


Figure 2. Vibration mode 2 of heat exchanger stands with strain energy plotted.

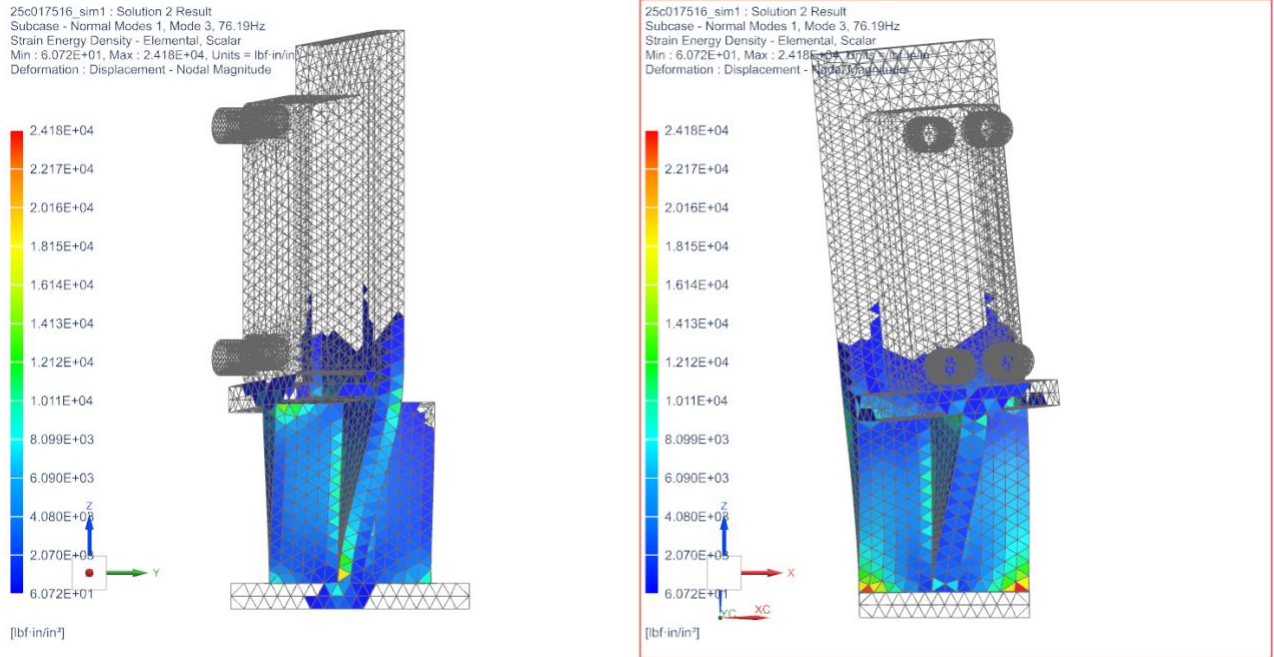


Figure 3. Vibration mode 3 of heat exchanger stands with strain energy plotted.

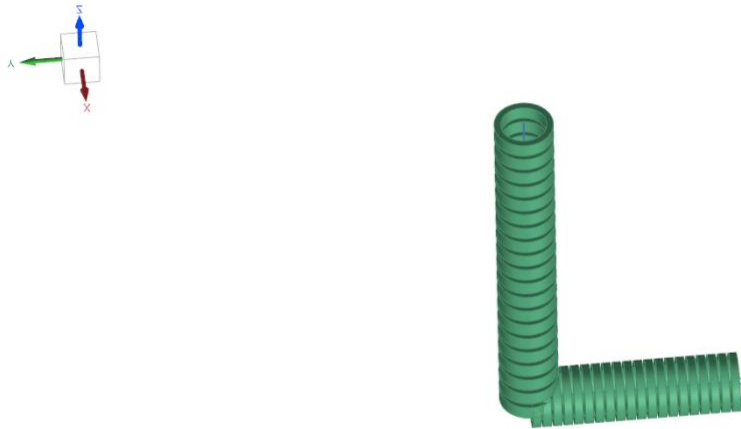


Figure 4: FEM setup of pipe modal analysis.

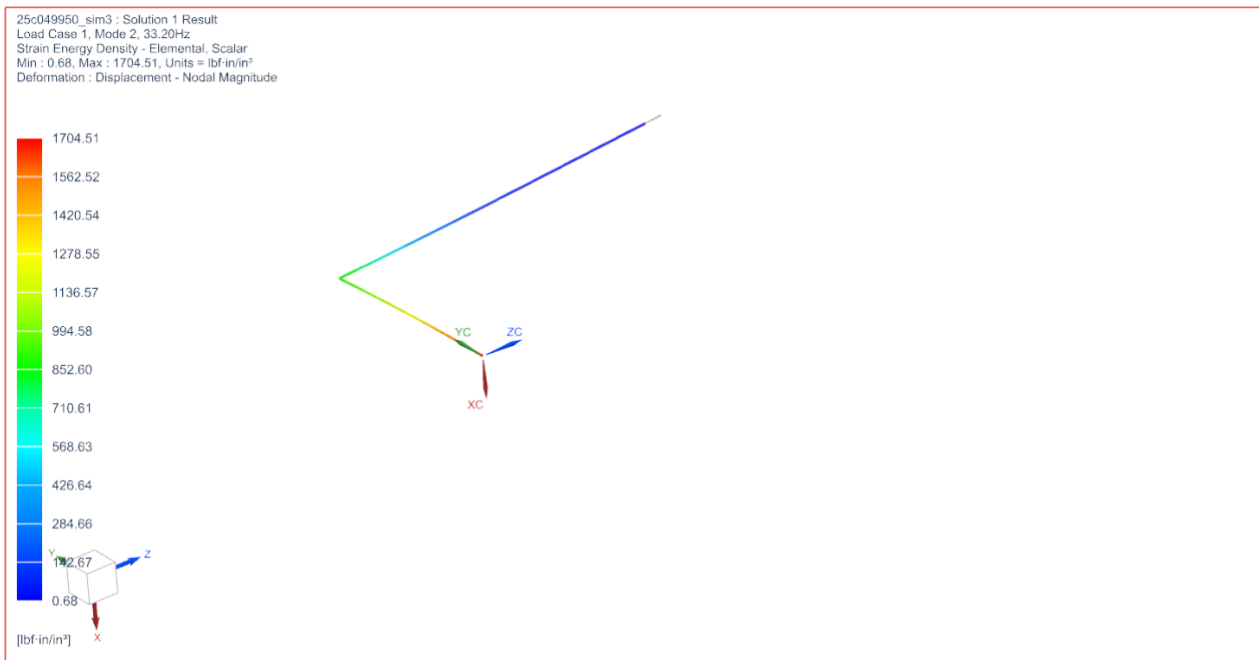


Figure 5. Strain energy plot of mode 2.

25c049950_sim3 : Solution 1 Result
 Load Case 1, Mode 3, 98.38Hz
 Strain Energy - Elemental, Scalar
 Min : 1.991E+00, Max : 1.818E+04, Units = lbf-in
 Deformation : Displacement - Nodal Magnitude



Figure 6, Strain energy plot of mode 3

APPENDIX C – CAD DRAWINGS

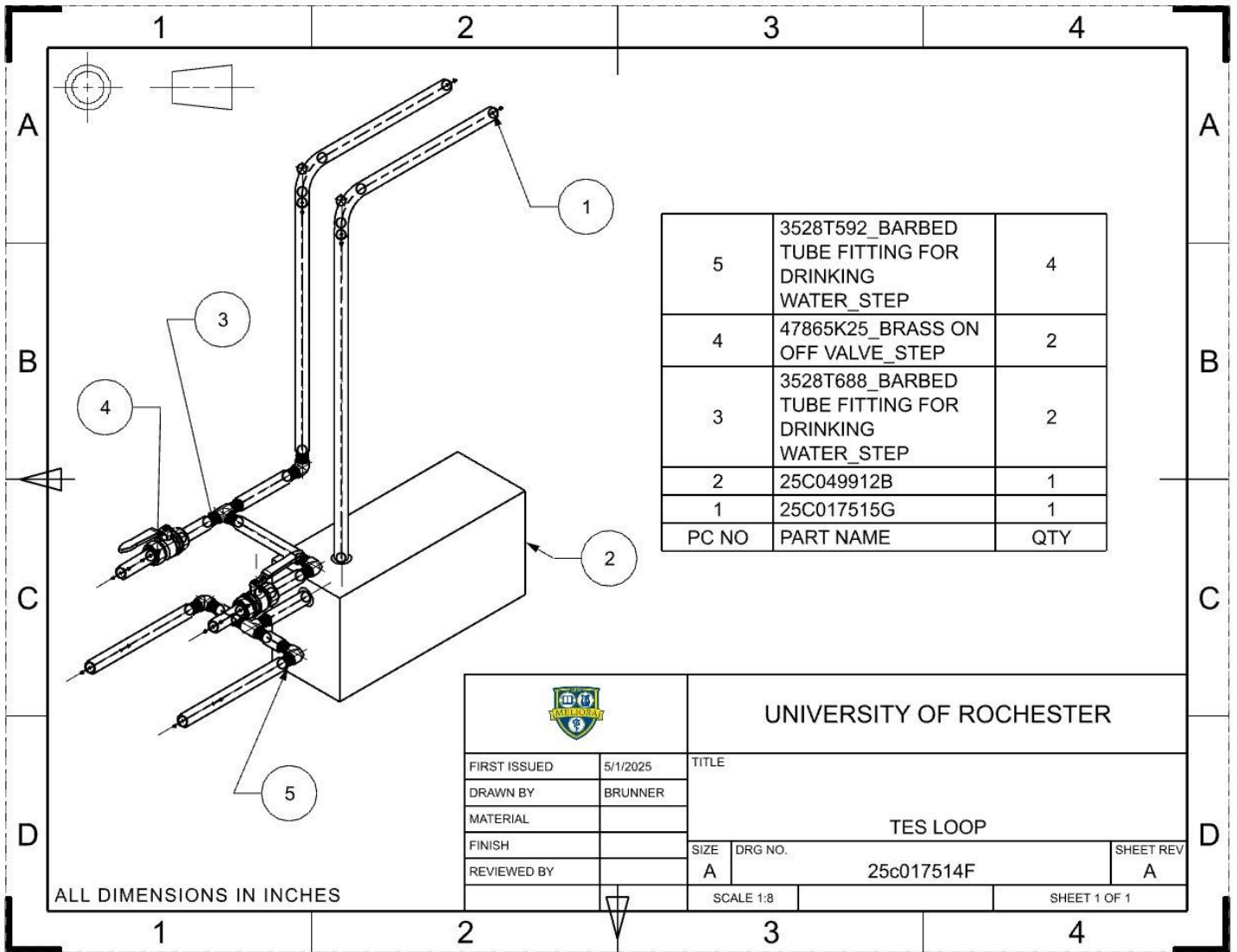


Figure 1. CAD drawing of finalized TES Loop.

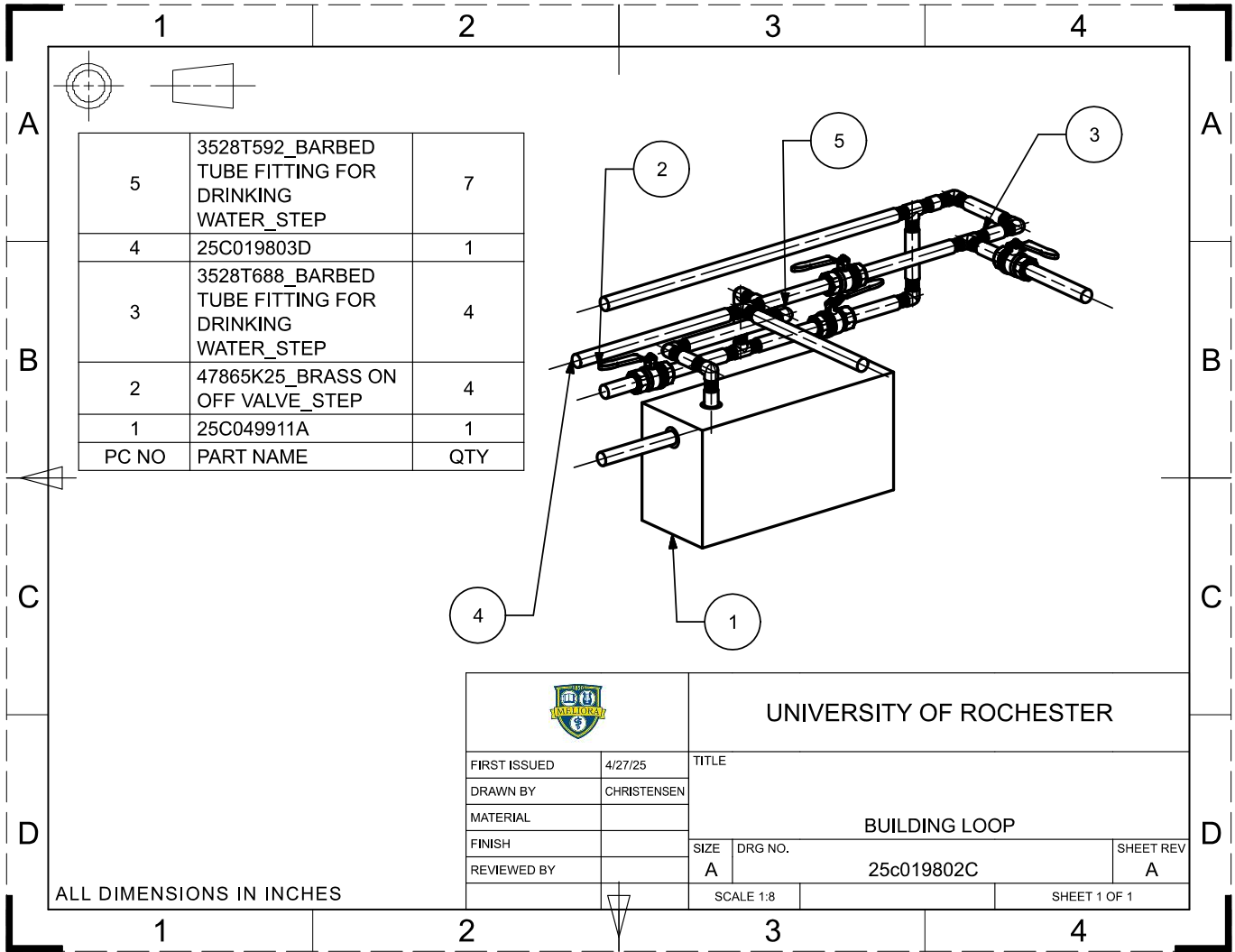


Figure 2. CAD drawing of finalized Building Loop.

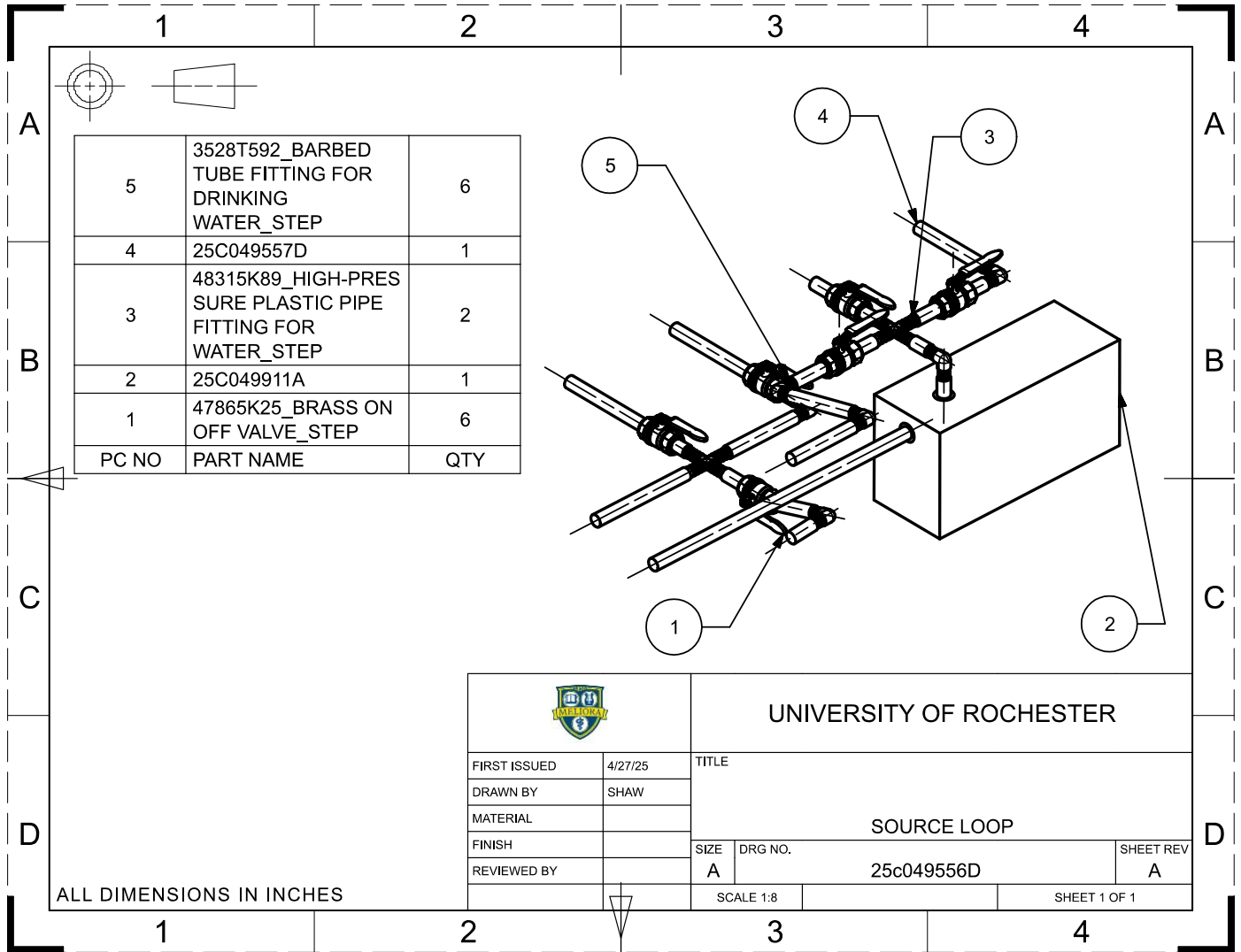


Figure 3. CAD drawing of finalized Source Loop.

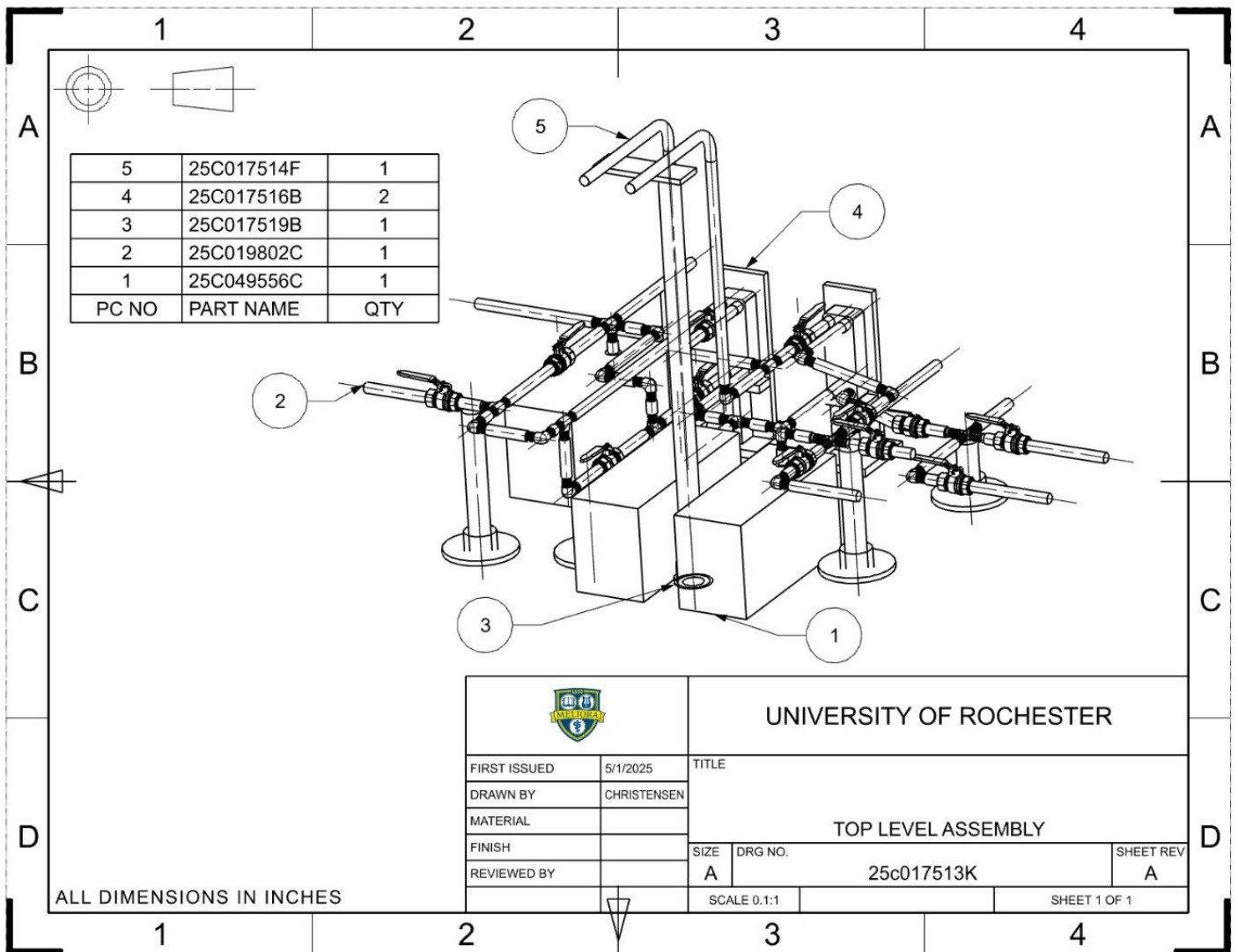


Figure 4. CAD drawing of finalized Top Level Assembly.